

# Wide-angle, nonmechanical beam steering with high throughput utilizing polarization gratings

Jihwan Kim,<sup>1</sup> Chulwoo Oh,<sup>1</sup> Steve Serati,<sup>2</sup> and Michael J. Escuti<sup>1,\*</sup>

<sup>1</sup>Department of Electrical and Computer Engineering, North Carolina State University, Raleigh, North Carolina 27695, USA

<sup>2</sup>Boulder Nonlinear Systems, Inc., Lafayette, Colorado 80026, USA

\*Corresponding author: mjescuti@ncsu.edu

Received 22 December 2010; accepted 12 February 2011;  
posted 21 March 2011 (Doc. ID 138643); published 6 June 2011

We introduce and demonstrate a ternary nonmechanical beam steering device based on polarization gratings (PGs). Our beam steering device employs multiple stages consisting of combinations of PGs and wave plates, which allows for a unique three-way (ternary) steering design. Ultrahigh efficiency (~100%) and polarization sensitive diffraction of individual PGs allow wide steering angles (among three diffracted orders) with extremely high throughput. We report our successful demonstration of the three-stage beam steerer having a 44° field of regard with 1.7° resolution at 1550 nm wavelength. A substantially high throughput of 78%–83% is observed that is mainly limited by electrode absorption and Fresnel losses. © 2011 Optical Society of America

*OCIS codes:* 050.1950, 060.4510, 090.1970, 230.1360, 260.5430.

## 1. Introduction

Nonmechanical beam steering promises substantial benefits to optoelectronic systems such as free-space laser communications, laser weapons, laser remote sensing, and fiber-optics; however, any viable solution must offer some or all of the following [1]: high throughput, rapid pointing ability, robustness to high intensity, and compact size. In order to achieve nonmechanical beam control, diverse approaches have been explored, including microlens arrays, electro-optic prisms, holographic glasses, and diffractive acousto-optic techniques. All of these approaches are, however, plagued by one or more of the following limitations: low throughput, scattering, small steering angle/aperture, and large physical size. Two recent efforts studied liquid crystal (LC) phase grating based continuous steering in two approaches: nonmechanical [2] and mechanical [3] steering. They demonstrated high efficiency and low leakage, but

they lack in rapid pointing ability for wide-angle steering.

In this work, we introduce a novel beam steering device based on the polarization-sensitive properties of LC polarization gratings (PGs) [4,5]. This single device is capable of diffracting incident light into one of three possible diffracted orders (0th and  $\pm 1$ st) according to the input polarization and the applied voltage. Based on a three-way (ternary) steering design of multiple stacked stages, we show that it is practical to achieve many dozen discrete steering angles, with high throughput (80%–95%) and with wide field of regard (e.g., 90°) compared to prior nonmechanical steering [6]. Since the PGs can be formed within thin LC cells and they are scalable to large areas without increasing their thickness, the device provides dramatic aspect ratio. Moreover, our device can be tailored to operate at nearly any wavelength from visible to midwave-IR. We show the beam steering device that performs nonmechanical wide-angle discrete steering of a laser beam (at 1550 nm). Our discrete beam steering technology can be combined with a fine-angle continuous steering for wide-angle continuous steering.

---

0003-6935/11/172636-04\$15.00/0  
© 2011 Optical Society of America

## 2. Background

The essence of our approach is a switchable nematic LC PG having continuous in-plane bend-splay patterns, shown in Fig. 1(a). The theoretical diffraction efficiencies of PGs can be expressed as [5]

$$\eta_0 = \cos^2(\Gamma/2), \quad (1a)$$

$$\eta_{\pm 1} = (1/2)(1 \mp S'_3) \sin^2(\Gamma/2), \quad (1b)$$

where  $\eta_m$  is the diffraction efficiency of the  $m$  order,  $\Gamma = 2\pi\Delta nd/\lambda$  is the retardation of the LC layer,  $\lambda$  is the wavelength of incident light, and  $S'_3 = S_3/S_0$  is the normalized Stokes parameter corresponding to the ellipticity of the incident light. Incident light is therefore diffracted into only one of the first orders when input is circular polarized ( $S'_3 = \pm 1$ ) and the retardation of the LC layer is half-wave ( $\Delta nd = \lambda/2$ ). Figure 1(b) shows a single steering stage that comprises a switchable wave plate (WP) and a switchable PG, resulting in three-way steering. When the input light is circularly polarized, the WP ensures that the input to the PG is either of the two orthogonal (left/right) circular polarization states. Depending on the handedness of polarization, the PG diffracts the beam into one of the first orders ( $+\theta$  or  $-\theta$ ) and flips its handedness. When voltage is applied on the PG ( $V \gg V_{th}$  [7], on-state PG), the grating profile is effectively erased (i.e.,  $\Delta n \approx 0$ ) and the incident beam passes through the PG, preserving its polarization state. The diffraction angle is established by the classic grating equation  $\theta_{out} = \sin^{-1}(m\lambda/\Lambda + \sin \theta_{in})$ , where the order  $m$  depends on the incident polarization and  $\Lambda$  is the grating period.

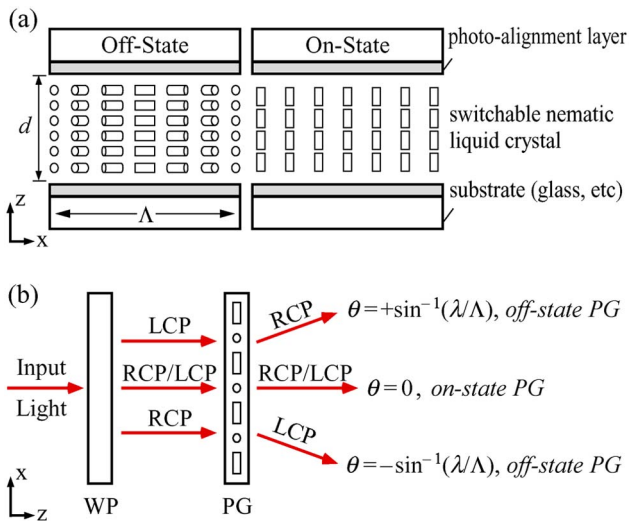


Fig. 1. (Color online) PG structure and single steering stage: (a) side view of a PG (on/off-state), showing LC director profile, (b) beam steering in single steering stage containing a WP and a PG, having different diffraction behavior with RCP and LCP incident light.

## 3. Operation Principles

Our ternary PG beam steering concept comprises multiple stacked stages of this WP/PG assembly. Figure 2(a) shows a ternary design (with  $N = 3$  stages), where each stage has a different grating period and can access a different set of angles. The most novel feature of this beam steerer is the fact of three possible steering directions of every stage, and the ability of each stage to add and subtract from the input angle (or leave it unchanged). Prior multistage diffractive approaches [8,9] comprised stages with only two output states (deflecting or not).

Our ternary PG design therefore enables far more angles to be steered by the same number of stages. The total number of steering angles  $M$  and angle resolution  $r$  are determined by the number of stages  $N$ :

$$M = 3^N, \quad (2a)$$

$$r = \text{FOR}/(3^N - 1), \quad (2b)$$

where FOR is the field of regard. We highlight the exponential increase of  $M$  in Fig. 2(b). The diffraction angle  $\theta_l$  and grating period  $\Lambda_l$  of each stage number  $l$  are

$$\sin \theta_l = \sin((3^l - 1)r/2) - \sin((3^{l-1} - 1)r/2), \quad (3a)$$

$$\Lambda_l = \lambda / \sin \theta_l, \quad (3b)$$

where  $\lambda$  is the wavelength of incident beam. The overall output angle  $\Theta$  can be expressed as

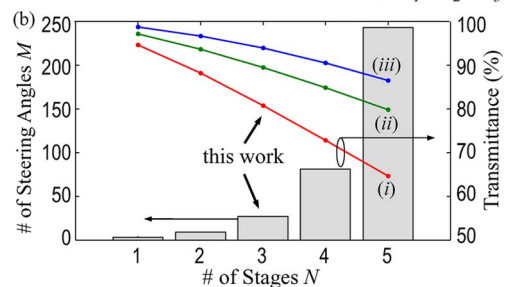
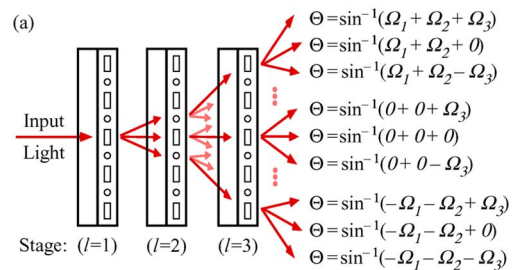


Fig. 2. (Color online) Ternary PG beam steering design: (a) three-stage ( $N = 3$ ) ternary steerer design has  $M = 27$  discrete steering angles (only 9 illustrated,  $\Omega_l = \sin \theta_l$ ), (b) number of steering angles and calculated transmittance versus number of stages. Three cases of  $\{\eta_{\pm 1}, D, R, A\}$  in Eq. (5) are shown, as described in the text.

$$\sin \Theta = \sum_{l=1}^N (-1)^{V_l^{\text{WP}}} V_l^{\text{PG}} \sin \theta_l, \quad (4)$$

where  $V_l^{\text{WP}}$  is the state of the  $l$ th WP (0 or 1 when the WP output is left-handed circular polarization [LCP] or right-handed circular polarization [RCP], respectively), and  $V_l^{\text{PG}}$  is the state of the  $l$ th PG (0 or 1 when  $V \gg V_{\text{th}}$  or  $V = 0$ , respectively).

If we assume that the PG efficiency and losses of each stage are the same, we can approximate the overall system transmittance  $T$  in the following way:

$$T = (\eta_{+1})^N (1 - D)^N (1 - R)^{2N} (1 - A)^{2N}, \quad (5)$$

where  $\eta_{+1}$  is the experimental intrinsic diffraction efficiency of each PG,  $D$  is the diffuse scattering of each PG, and  $R$  and  $A$  are the Fresnel reflectance and absorption losses, respectively, of each LC cell.

We graph  $T$  for three cases in Fig. 2(b). Case (i) corresponds to the parameters we were able to experimentally demonstrate in this work (i.e.,  $\eta_{+1} \approx 99.6\%$ ,  $D = 0.3\%$ ,  $R = 1.2\%$ , and  $A = 1.0\%$ ), where simple indium-tin-oxide (ITO) electrodes were implemented. Case (ii) corresponds to the case in which commercially available index-matched ITO electrodes are used, to reduce to  $R = 0.1\%$ . Case (iii) corresponds to the best-case scenario, where low loss transparent conductors are employed to reach  $A = 0.2\%$ , the performance expected from Transcon 1000  $\Omega/\text{sq}$  conductors [1]. In all cases, we observe a roughly linear decrease in  $T$  as  $N$  increases. However, we simultaneously observe an exponential increase in  $M$ , a very favorable scaling behavior. For a reasonably large number of steering angles,  $25 \leq M \leq 100$ , we predict  $72\% \leq T \leq 94\%$ , primarily depending on the sophistication of the electrodes.

#### 4. Fabrication and Results

To demonstrate this steering concept, we prepared three PGs using polarization holography [6], commercial materials, and standard LC cell processing. We utilized a linear photopolymerizable polymer (LPP) (ROP-103/2CP, from Rolic) as the photoalignment material and orthogonal circularly polarized beams from a He-Cd laser (325 nm) to record the PG pattern. A  $\sim 2.5 \mu\text{m}$  cell thickness was achieved with glass spheres (Dana Enterprises) to set half-wave effective retardation with the nematic LC (LCMS-102, from Boulder Nonlinear Systems,  $\Delta n = 0.31$  measured [10] at 1550 nm). To minimize reflection loss, all LC elements were laminated to each other with optical glue (NOA-63, Norland), and glass with antireflection coatings (PG&O) was glued to the front and back faces. The parameters  $\Lambda_l$  and  $\theta_l$  of each PG were chosen according to Eq. (3) and are listed in Table 1. The three WPs were fabricated in a similar fashion, but with uniformly aligned LPP layers.

Table 1 shows characterization data of the individual PGs with an infrared laser (1550 nm, 40 mW). In

Table 1. Individual PG Characterization Data

$l$ (stage)	$\theta_l$ (deg)	$\Lambda_l$ ( $\mu\text{m}$ )	$D_l$ (%)	$\eta_{+1}$ (%)
1	1.7	52.6	0.0	99.9
2	5.1	17.5	0.3	99.8
3	14.9	6.0	1.6	99.7

order to obtain an experimental quantity  $\eta_{+1}$  comparable to Eq. (1b), we define the intrinsic diffraction efficiency of order  $m$  as  $\eta_m = P_m / (P_{-1} + P_0 + P_{+1})$ , where  $P_m$  is the measured power of the  $m$ th diffraction order, when the input is circularly polarized. We define the scattering loss  $D$  as the fraction of transmitted light (measured using an integrating sphere) that does not appear within one of the three diffraction orders. These PGs exhibit nearly ideal diffraction properties so that  $\geq 99.7\%$  of light is steered into the intended direction without observable higher orders ( $\eta_0 \leq 0.2\%$ ,  $\eta_{m \geq 2} < 0.05\%$ ).

We assembled a prototype ternary beam steerer containing three steering stages, which covered  $44^\circ$  FOR with  $1.7^\circ$  resolution at 1550 nm wavelength. In Fig. 3(a), we show the relative transmitted power across the observed output angle range  $\pm 30^\circ$  for two steered direction settings:  $-22^\circ$  (all PGs diffracting) and  $0^\circ$  (all PGs nondiffracting). The only significant sidelobe ( $\sim 0.8\%$ ) appears at  $-6.8^\circ$  for the diffracting case. This leakage relates to the oblique incidence on the last PG ( $l = 3$ ) and likely can be reduced by the use of higher birefringence LC and additional retardation compensation films. Very low sidelobes are generally observed throughout the steering range, as shown in the inset picture of Fig. 3(a).

The measured diffraction efficiency and transmittance of the mainlobe are shown in Fig. 3(b). The

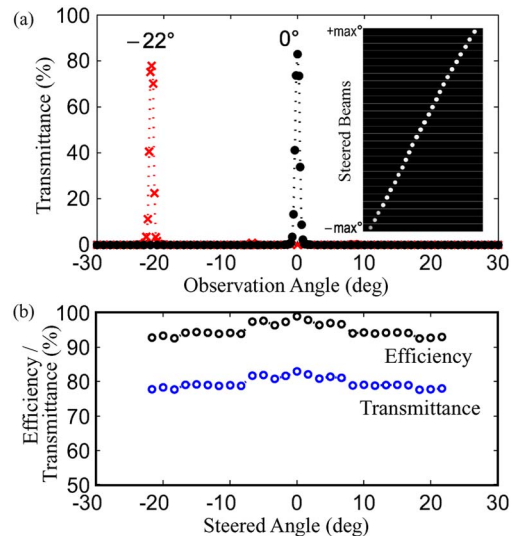


Fig. 3. (Color online) Measured output of the  $N = 3$  ternary PG steerer operating at 1550 nm: (a) relative power (i.e., transmittance) at all output angles for two intended mainlobe steering angles ( $-22^\circ$  and  $0^\circ$ ) (inset: composite image of photographs of the 27 steered beams on an IR viewing card), (b) transmittance and diffraction efficiency of the mainlobe for all steering angles.

measured transmittance, comparable to Eq. (5), is calculated as  $T = P_{\text{main}}/P_{\text{in}}$ , where  $P_{\text{main}}$  is the mainlobe power and  $P_{\text{in}}$  is the input power. The efficiency, a normalization that removes the effect of the substrates to reveal the aggregate effect of the diffractive PGs, is defined as  $\eta = P_{\text{main}}/P_{\text{tot}}$ , where  $P_{\text{tot}}$  is the total transmitted power into the exit hemisphere, measured with an integrating sphere. For all steering angles, solid transmittance (78%–83%) was observed, along with high diffraction efficiency (94%–99%). This confirms that losses in this demonstration are predominantly related to the substrate absorption and reflection and that the PGs are fairly efficient at redirecting light as expected, even when the incidence angle is far from the normal direction.

## 5. Conclusion

In summary, we demonstrated a PG-based, wide-angle, nonmechanical beam steerer having 44° FOR with 1.7° resolution at 1550 nm and described its design principles. The device shows high optical throughput (78%–83%) that can be substantially improved by optimizing substrates and electrode materials. This ternary PG beam steerer offers exponential scaling ( $3^N$ ) of the number of steering angles, can achieve very low sidelobes, and supports comparatively large beam diameters paired with a very thin assembly and low beam walk-off. The size of the PGs depends almost entirely on the size of the optics in the holographic setup, and we have made up to the range of 6 in fairly easily. Moreover, PG fabrication is relatively easier and more cost-effective compared to other conventional approaches in this context. Note that while the results and design described here are limited to steering in one dimension, two-dimensional steering could be implemented by

arranging two of these PG steering assemblies sequentially (i.e., one for azimuth, one for elevation).

The authors acknowledge support from the U.S. Air Force Research Laboratory (Sensors Directorate) and productive discussions with Paul McManamon.

## References

1. P. F. McManamon, P. J. Bos, M. J. Escuti, J. Heikenfeld, S. Serati, H. Xie, and E. A. Watson, "A review of phased array steering for narrow-band electrooptical systems," *Proc. IEEE* **97**, 1078–1096 (2009).
2. L. Shi, P. F. McManamon, and P. J. Bos, "Liquid crystal optical phase plate with a variable in-plane gradient," *J. Appl. Phys.* **104**, 033109 (2008).
3. C. Oh, J. Kim, J. Muth, S. Serati, and M. J. Escuti, "High-throughput continuous beam steering using rotating polarization gratings," *IEEE Photon. Technol. Lett.* **22**, 200–202 (2010).
4. J. Tervo and J. Turunen, "Paraxial-domain diffractive elements with 100% efficiency based on polarization gratings," *Opt. Lett.* **25**, 785–786 (2000).
5. C. Oh and M. J. Escuti, "Numerical analysis of polarization gratings using the finite-difference time-domain method," *Phys. Rev. A* **76**, 043815 (2007).
6. J. Kim, C. Oh, M. J. Escuti, L. Hosting, and S. Serati, "Wide-angle nonmechanical beam steering using thin liquid crystal polarization gratings," *Proc. SPIE* **7093**, 709302 (2008).
7. R. K. Komanduri, W. M. Jones, C. Oh, and M. J. Escuti, "Polarization-independent modulation for projection displays using small-period LC polarization gratings," *J. Soc. Inf. Disp.* **15**, 589–594 (2007).
8. X. Wang, D. Wilson, R. Muller, P. Maker, and D. Psaltis, "Liquid-crystal blazed-grating beam deflector," *Appl. Opt.* **39**, 6545–6555 (2000).
9. O. M. Efimov, L. B. Glebov, and V. I. Smirnov, "High-frequency Bragg gratings in a photothermorefractive glass," *Opt. Lett.* **25**, 1693–1695 (2000).
10. M. J. Escuti, D. R. Cairns, and G. P. Crawford, "Optical-strain characteristics of anisotropic polymer films fabricated from a liquid crystal diacrylate," *J. Appl. Phys.* **95**, 2386–2390 (2004).